Pergamon

Journal of Structural Geology, Vol. 17, No. 7, pp. 1047 to 1053, 1995

0191-8141/95 $9.50 + 0.00

0191-8141(94)00121-9

Effects of strain gradients on asymmetry of experimental normal fault systems

MASAHIRO ISHIKAWA* and KENSHIRO OTSUKI

Department of Geoenvironmental Science, Faculty of Science, Tohoku University, Aobayama, Sendai 980-77, Japan

(*Received* 15 *September* 1993; *accepted in revised form* 24 *October* 1994)

Abstract—Sandbox experiments were carried out to investigate the influence of horizontal strain gradients on the asymmetry of normal fault systems in regions of crustal extension. During the experiments, faults facing in the direction of higher strain were preferentially developed. The results show that the horizontal strain gradient is an important factor in controlling the asymmetry of normal fault systems. The experiments also relate the degree of asymmetry to the horizontal strain gradient. The results may be applicable to the formation of asymmetric normal fault systems on either side of the axes of mid-oceanic ridges, extensional back-arc regions, and continental rifts.

INTRODUCTION

Horst/graben and half-graben systems are the two principal modes of brittle crustal deformation during extensional tectonics. They differ geometrically depending on whether the two fault groups of a conjugate normal fault set are equally developed (symmetric) or one group is selectively formed (asymmetric). Possible theories of faulting, however, do not predict the asymmetry. Coulomb–Navier's criterion for shear failure, for example, only can determine two potential fault planes which are symmetric to the principal stress axes (Jaeger & Cook 1979).

In recent years, many analogue model experiments have been carried out to model crustal rifting and extensional fault systems (Crans *et al.* 1980, Brun & Choukroune 1983, McClay & Ellis 1987a,b, Vendeville *et al.* 1987, Ellis & McClay 1988, Kautz & Sclater 1988, Mandl 1988, Vendeville & Cobbold 1988, McClay 1990a,b, Allemand & Brun 1991, Buchanan & McClay 1991, McClay & Scott 1991, Tron & Brun 1991). In sandbox experiments designed to model uniform extension (Brun & Choukroune 1983, Vendeville *et al.* 1987, McClay & Ellis 1987a,b), horst/graben systems were formed. McClay & Ellis (1987a), Vendeville *et al.* (1987) and Vendeville & Cobbold (1988) carried out the sandbox experiments on a gently inclined plane, resulting in a half-graben system. The results are consistent with asymmetric patterns of extensional fault systems in continental rifts associated with a large low angle normal fault proposed by Wernicke (1981, 1985) and Wernicke & Burchfiel (1982). As pointed out by Vendeville & Cobbold (1988), the component of shear force parallel to the inclined plane due to the gravitational body force may be a cause of asymmetric development of normal faults. The shear force and the frictional force on the rubber sheet may produce a gradient of tensional stress in the sand layers. However, McClay (1990a) presented two special conditions for the formation of asymmetric normal fault systems without the use of an inclined plane. In this paper, we model asymmetric normal fault systems without extending above an inclined plane. We report the dependency of the asymmetry of experimental normal fault systems on the horizontal strain gradient which was controlled artificially in the sandbox.

EXPERIMENTAL METHOD

A sandbox 44 cm long and 36 cm wide was used to make the experiments (Fig. 1). The condition of sand packing was fixed in each experiment by using a constant mass of sieved round glass sand (0.5 mm in diameter) and by making layers of 9.5 cm in total thickness above a rubber sheet. Marker layers of coloured glass sand of the same size were interbedded. The rubber sheet is

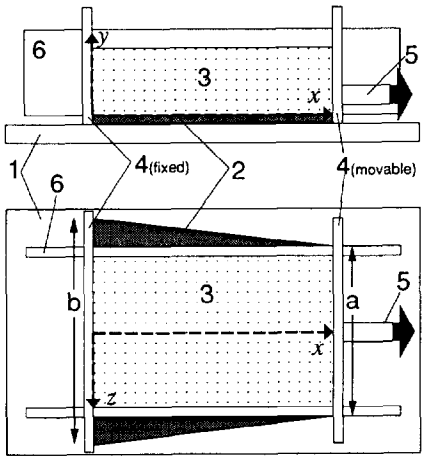

Fig. 1. Plan and cross-section of the sand-box, showing coordinate systems used. 1: Rigid base, 2: rubber sheet, 3: sand layer, 4: fixed wall (left) and movable wall (right), 5: worm screw, 6: acrylic walls.

*Present address: Department of Earth Science, National Institute of Polar Research, 9–10 Kaga 1-Chome, Itabashi-ku, Tokyo 173, Japan.

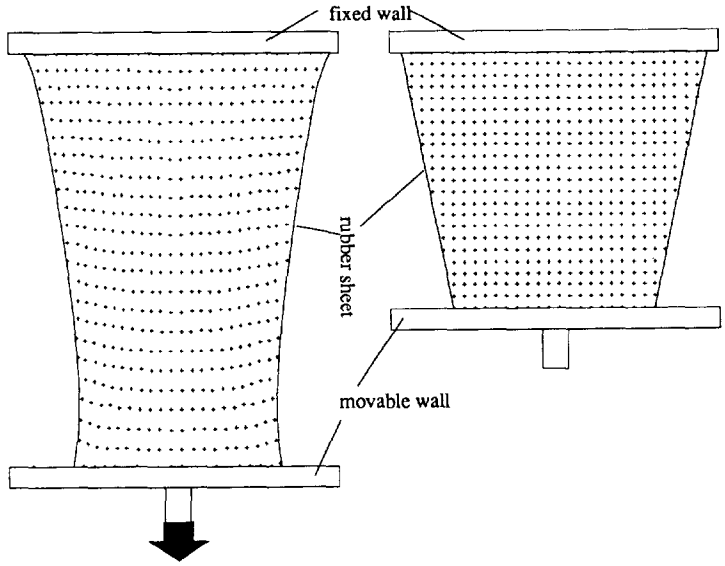

Fig. 2. Grid pattern on rubber sheet in the undeformed (right) and deformed (left) states.

stretched by moving one side wall (a) outward by hand-controlled worm screw. The wall velocity was slower than 40 cm min^{-1} to avoid slipping between the sand layer and rubber sheet.

The key point of our experiments is to make and control a gradient in the horizontal extensional strain. In order to produce the strain gradient, we used a trapezoidal rubber sheet 44 cm long, 38 cm wide on one side (a) and various widths (38, 42, 48, 58, 90 cm) on the other side (b). The horizontal strain gradient can be controlled by changing the ratio b/a. The coordinates (x, y, z) are set up on the rubber sheet as shown in Fig. 1. The deformed state will be described by reference to the coordinates in the undeformed state (i.e. a Lagrangian description). The extensional strain was measured by the grid markers drawn on the sheet. Here we use extensional strain ε_x defined as $(l\text{-}l_0)/l_0$, where l_0 and l are the width of grid in the undeformed and deformed states, respectively.

Figure 2 shows the deformed shape of the grid which was square before stretching. It should be noted that the strain state is not uniform because a and b are kept constant throughout stretching the rubber. Figure 3 shows the change in ε_x of the rubber sheet with $a = 38$ cm and $b = 58$ cm when the rubber stretching = 4, 10, 16 and 22 cm. The change in ε_x along the axial line ($z = 0$) is different from that along a marginal line ($z = 18$ cm). In the region where $x < c$. 32 cm, ε_x in the marginal part is smaller than in the axial part, while this relation is reversed in the region where $x > c$. 32 cm. It is notable that the strain gradient $d\varepsilon_x/dx$ along the axial line becomes negative in the region where $x > c$. 32 cm. However, the averaged strain of the axial and marginal parts increases nearly in proportion to x. In addition, both the averaged strain at any value of x and the strain gradient averaged throughout x are nearly proportional to the amount of rubber stretching.

Figure 4 shows strain measured along the marginal line ($z = 18$ cm) of the rubber sheet of $b = 58$ cm overlain by a 9.5 cm thick sand layer when the total extension is 16 cm. Comparing the extensional strain ε_x of Fig. 4 with ε_x without the sand layer (Fig. 3), ε_x in Fig. 4 becomes smaller than that of Fig. 3 in the range of $x < 20$ cm, and larger than that of Fig. 3 in the range of $x > 20$ cm. This

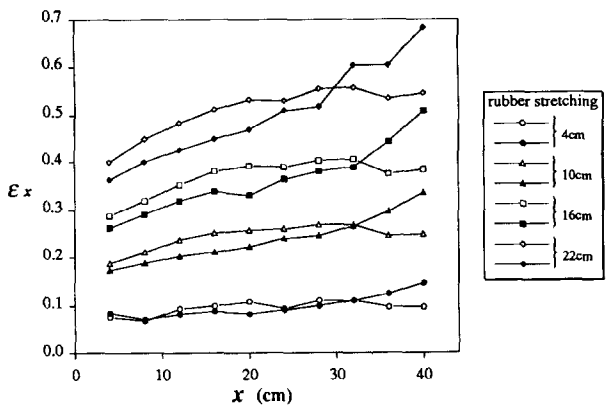

Fig. 3. The relation between extensional strain ε_x of rubber sheet and the x-coordinate when rubber is stretched by 4, 10, 16, 22 cm. The open and solid symbols denote the strains measured along the axial line ($z = 0$) and the marginal line ($z = 18$ cm).

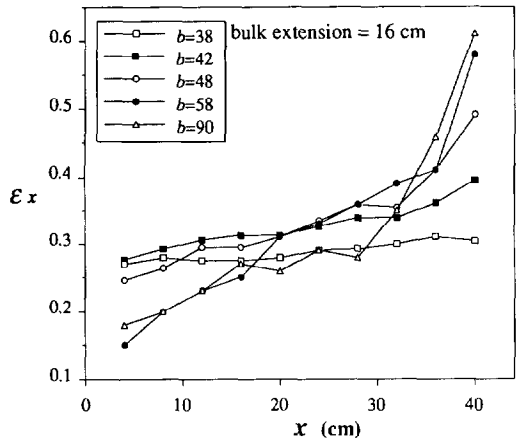

Fig. 4. The relation between extensional strain ε_x of rubber sheet overlain by 9.5 cm thick sand layer and x-coordinate when the rubber sheets with $a = 38$ cm and $b = 38, 42, 48, 58, 90$ cm are stretched by 16 cm.

comparison shows that the extensional strain gradient of the rubber sheet overlain by a sand layer is larger than that of the rubber sheet without a sand layer. Even in the case of $a = b = 38$ cm, the strain gradient is not zero but slightly positive. Strain is concentrated, especially in the cases of $b > 48$ cm, in the region $x > 30$ cm; that is, we consider that the sand layer causes the larger strain gradient, and that the difference in strain gradient is due to the effect of friction between the rubber sheet and rigid base. Figure 4, however, displays the dependency of the strain gradient on the b length.

Gaps which are not filled by sand appear between the side walls and the ends of the sand layer, but they are very narrow. Therefore, slipping between the rubber sheet and the base of sand layer is negligible, and the strain in the rubber sheet is thought to be transmitted faithfully to the sand layer.

The deformation process was recorded by time-lapsed photography of the free upper surface and the side surface through a transparent acrylic wall. The deformation of the sand layer is more or less affected by the friction along the acrylic walls which are fixed to the movable side wall (a). To avoid this effect, fault throw and fault number were measured on the upper surface along the axial line of the apparatus by micrometer.

EXPERIMENTAL RESULTS

General characteristics of faulting process

Figure 5 shows the faulting process in the case of $a = 38$ cm and $b = 90$ cm as an example. While the stretching of the rubber sheet is less than 4 cm, the sand layer is extended mainly by flow with few faults. The very narrow gaps, which become narrower downward, occur between the a and b side walls and the ends of the sand layer, and they imply that the lateral flow is slightly greater in the lower sand layer than the upper layer. When the total extension is 6 cm, several conjugate normal faults are formed in the upper sand layer around the region of $x = 38$ cm (coordinate in undeformed state) where extensional strain along the axial part of the rubber sheet is expected to be a maximum (see Fig. 3). Brittle faulting with narrow shear zones and sharp fault traces is restricted to the uppermost part of the sand

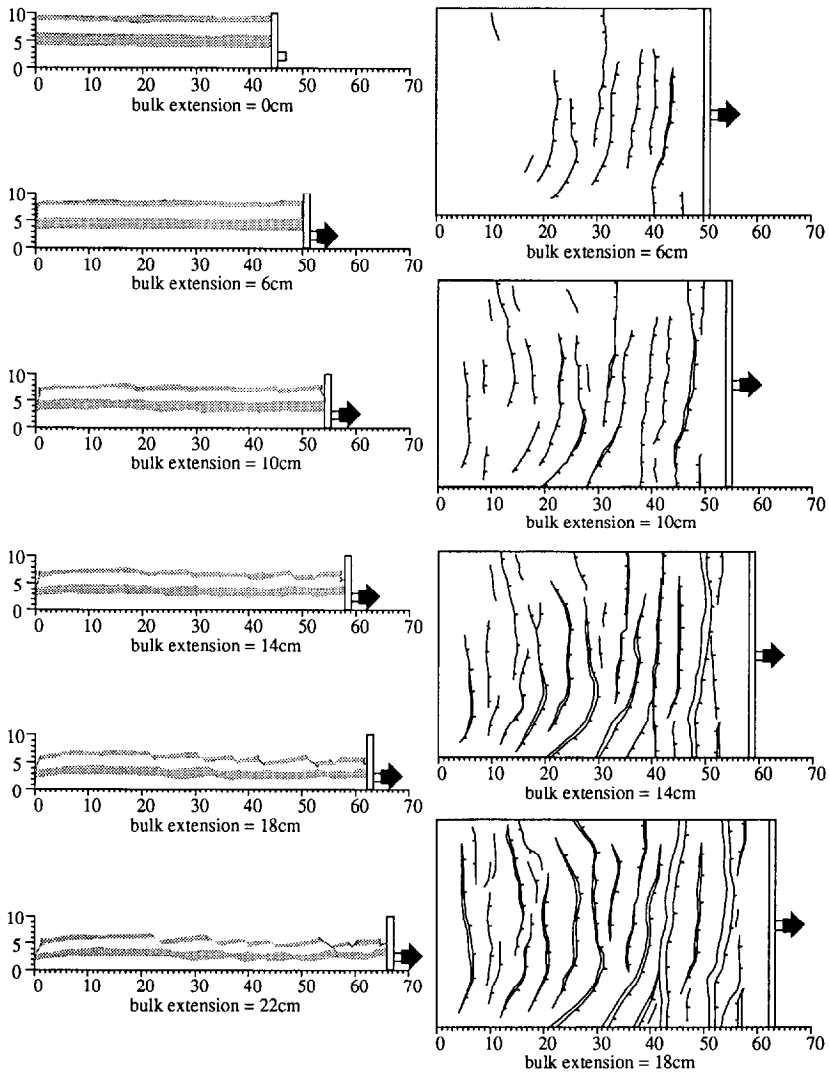

Fig. 5. An example of the deformation of the sand layer during an experiment with $a = 38$ cm and $b = 90$ cm. The left and right are side and top views, respectively.

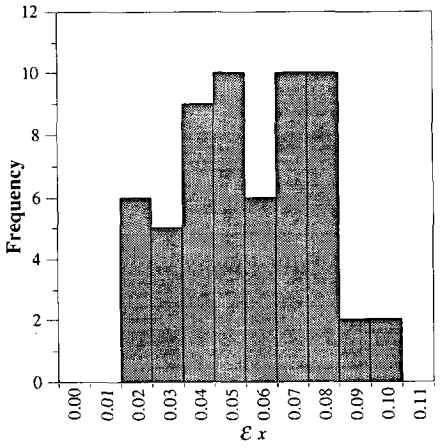

Fig. 6. The relationship between the frequency of initial faulting and the extensional strain ε_x at the faulting site.

layer. As the amount of stretching increases, new fault generation and the widening of the faulted region take place successively toward the lower strained side (left) which is about 3–5 cm distant from the front of the faulted region. The faults grade downward into wide ductile shear zones which are recognized by undulations of the marker sand layers, and they converge on the basal plane of the sand layer. The wavelength of the undulations is nearly equal to the fault spacing, suggesting a fault-related plastic flow.

The magnitude of strain at the inception of faulting ranges mostly from 0.02 to 0.08 as shown in the histogram of the frequency of the initial faulting against horizontal strain (Fig. 6). The dip angle of fault planes, about 70° at the initial stage of deformation, decreases gradually with the rotation of faulted blocks.

As mentioned already, faulting in the upper part of the sand layer is preceded by flow especially in the lower part. Therefore, the growth of faults is considered to involve the concentration of penetrative flow in the lowermost part of the sand layer into narrower zones and brittle faults in the upper part.

Increase in fault number and fault throw

The migration of the front of the faulted region occurs by nucleation of a new fault ahead of the zone so that the total number of faults increases as stretching of the rubber sheet is advanced. The number of faults also increases by the intercalation of a new fault between old faults. However, faults do not increase in number uniformly, but reach an optimum (about 11) at 6 to 10 cm bulk extension, being independent of ratio b/a. The total number of faults increases slightly thereafter, and attains a maximum of 12 to 16 at 22 cm bulk extension. Such non-linear increase of fault number is equally common for both fault groups of the conjugate set.

In contrast to the non-linear relationship between fault number and the amount of bulk extension, the total throw of all faults depends linearly on it; the proportional coefficient is 6.33, 5.64, 8.27, 5.15 mm cm^{-1} when b is 42, 48, 58, 90 cm. The deviation of the coefficients may be due to the change in frictional coefficient of sand grain surfaces which is affected by air humidity and the initial packing condition of sand grains, although we cannot explain the reason in detail. The smaller the coefficient is, the more the deformation may be partitioned to flow rather than faulting. The linear dependency of total throw on the amount of rubber stretching is characteristic of both conjugate fault groups.

Asymmetry of normal fault system

Fault planes dip preferentially toward the more highly strained side and are associated with a graben in the area of highest strain (Fig. 5), suggesting that the strain gradient affects the asymmetric development of conjugate normal faults. Here we define the asymmetries An and At of fault system as:

$$An = \frac{Tn_1}{Tn_1 + Tn_2} \tag{1}$$

and

$$At = \frac{Tt_1}{Tt_1 + Tt_2} \tag{2}$$

where Tn_1 and Tt_1 are the total number and total throw of the faults facing in the direction of increasing strain and Tn_2 and Tt_2 are those of fault planes dipping in the opposite direction.

We further define mean values of asymmetries An and At for about ten experiments under the same conditions:

$$\text{mean value of } An = \frac{\sum_{i=1}^{p} Tn_{1_i}}{\sum_{i=1}^{p} (Tn_{1_i} + Tn_{2_i})} \tag{3}$$

and

$$\text{mean value of } At = \frac{\sum_{i=1}^{p} Tt_{1_i}}{\sum_{i=1}^{p} (Tt_{1_i} + Tt_{2_i})} \tag{4}$$

where p means the total numbers of experiments made under the same conditions. As mentioned already, we can control the strain gradient $d\varepsilon_x/dx$ by changing b/a. In order to make clear the dependency of An and At on b/a or $d\varepsilon_x/dx$, the faults in the region $38 < x < 44$ cm where the strain gradient is negative are excluded from the discussions below.

Asymmetries An and At fluctuated during the first 10 cm of bulk extension, and became stable gradually thereafter. Mean values of asymmetries An and At also behave in the same way (Fig. 7). Figure 8 shows the dependencies of An and At on b (a is constantly 38 cm) at 16 cm bulk extension when asymmetries An and At are relatively stable. These values show large deviations in ten experiments under the same b condition. This is a reasonable result, because faulting is essentially a sto-

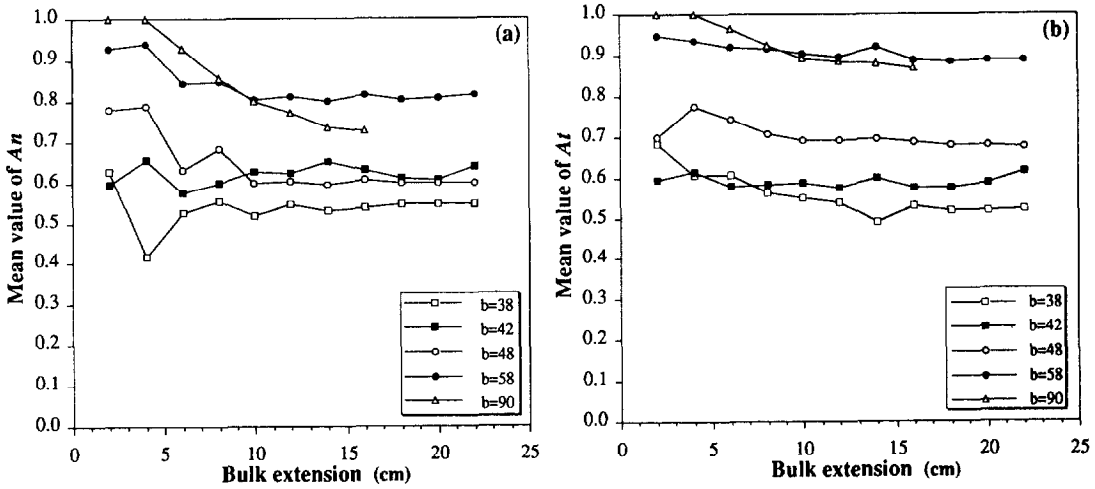

Fig. 7. The relations of the mean values of the fault asymmetries An (a) and At (b) obtained from about ten experiments under the same conditions of bulk extension in cases of a = 38 cm and b = 38, 42, 48, 58, 90 cm.

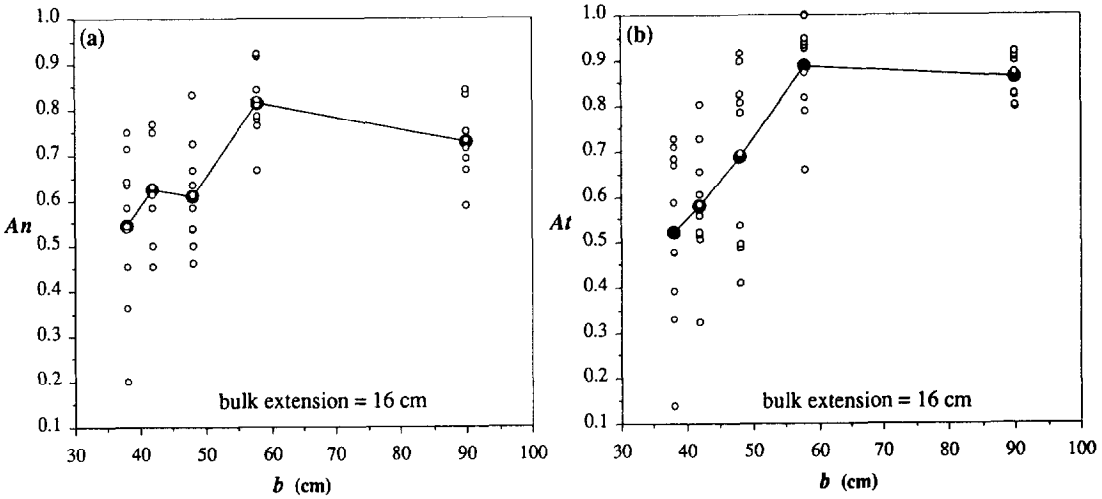

Fig. 8. The dependency of the fault asymmetries An (a) and At (b) on the length b for a bulk extension of 16 cm. Solid circles denote mean values of An and At for about ten experiments under the same conditions.

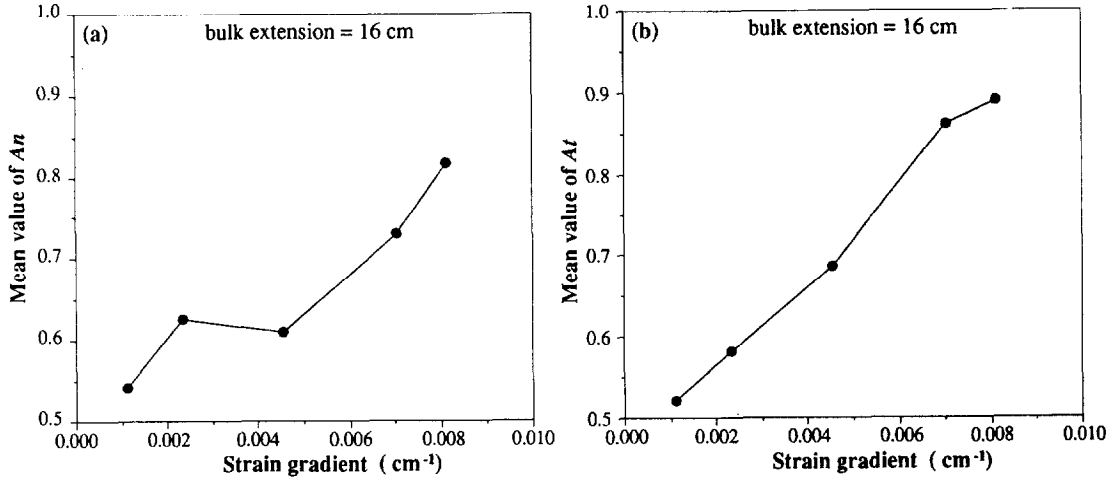

Fig. 9. The dependency of the fault asymmetries An (a) and At (b) on strain gradient when the bulk extension = 16 cm. The mean values of asymmetries An and At are averages for about ten experiments under the same conditions. It should be noted that the order of plots at b = 58 cm and b = 90 cm is reversed. This is due to the mean strain gradient in the region $x <$ 38 cm at b = 90 cm being just smaller than that at b = 58 cm (Fig. 4).

chastic process. The deviations become smaller as b increases, suggesting that the stochastic effect is depressed effectively by increasing the deterministic parameter b. In spite of the large deviations, the average values, both of An and At, show positive correlations with b, except for the case of $b = 90$ cm.

By using strain values in the region $x < 38$ cm (Fig. 4), the data can be replotted as the relations between the fault asymmetries and the mean strain gradient (Fig. 9). The results in Fig. 9 have not enough accuracy to determine the form of function, but they show positive correlations between the fault asymmetries and strain gradient. Here we should note again that we use the strain values measured at the margin of the rubber sheet in Fig. 4 to estimate strain gradients.

In order to investigate the effect of movement direction on the fault pattern produced, experiments were performed by moving: (1) the b side wall; and (2) both side walls with a variety of b lengths. Under these conditions as well, the faults tend to face to the more highly strained side preferentially. Therefore these results suggest that the horizontal extensional strain gradient is an effective parameter in determining the asymmetry of normal fault systems. Moreover, two supplementary sandbox experiments were made in order to check the effect of uneven thickness of the sand on the fault asymmetries by using the rubber sheet of $a = 38$ cm and $b = 90$ cm. In one experiment, sand is supplied to the depressed surface of the thinned sand layer, keeping the surface flat during the rubber stretching. In another experiment, a tapered sand layer was used with an initial surface of 6°. However, any significant differences in fault asymmetries from the ordinary experiments were not detected.

DISCUSSIONS AND CONCLUSIONS

Both continental rifts (e.g. Basin and Range province—Wernicke 1981, Smith & Bruhn 1984; Scottish mainland and its western continental shelf—Kirton & Hitchen 1987, Cheadle *et al.* 1987; North Sea—Ziegler 1982a, White & McKenzie 1988; North China Plain—Liu 1987) and mid-oceanic ridges (Harper 1985) have a common geometric feature: systematic half-grabens with fault asymmetry, nearly equidistant fault spacing, and tilting of fault blocks. Such geometric characteristics are well simulated by our sandbox experiments.

Two modes of crustal deformation during rifting are recognized: a pure shear model in which the crust is uniformly stretched (McKenzie 1978) and a simple shear model in which the crust is stretched by a low angle normal fault (Wernicke 1981, 1985, Wernicke & Burchfiel 1982). According to this study and extensional analogue model experiments by other geologists (Brun & Choukroune 1983, Vendeville *et al.* 1987, McClay & Ellis 1987a,b), uniform bulk extension (the pure shear model) results in development of horst/graben structures. On the other hand, half-graben systems were simulated when sand layers were stretched above a gently inclined base (McClay & Ellis 1987a, Vendeville *et al.* 1987, Vendeville & Cobbold 1988), which is equated with the low angle normal fault of the simple shear model. In some rift zones mentioned above, normal faults converge on a large low angle normal fault at crustal depth, and the latter experiments appear to support the simple shear model for rifting. In addition, McClay (1990a) simulated half-graben systems by extension above: (1) a basal detachment which undergoes stretching over a limited area; and (2) a basal detachment which undergoes stretching under the whole model and which has no constraints at the ends. However, our experiments corroborate that the strain gradient is an effective, quantitative parameter which determines whether horst/grabens or half-grabens develop. The low angle normal fault of the simple shear model may be a special but non-unique mechanism of producing an increase in strain down-dip necessary for the formation of synthetic listric normal faults in the hanging wall. In our experiments, the flow zone in the lowermost part of the sand layer may correspond to the low angle normal fault.

While direct measurements of strain gradients in extensional tectonic zones are not available , at least two plausible mechanisms exist to produce an extensional strain gradient in the lithosphere. One is due to the shear stress on the basal surface of the lithosphere caused by asthenospheric flow during active rifting (Sengör & Burke 1978, Condie 1989). When the active upwelling asthenospheric flow diverges laterally, the extensional stress and strain in the lithosphere are a maximum at the axis and decrease laterally (Fig. 10a). A second possible cause of a strain gradient is the uneven mechanical

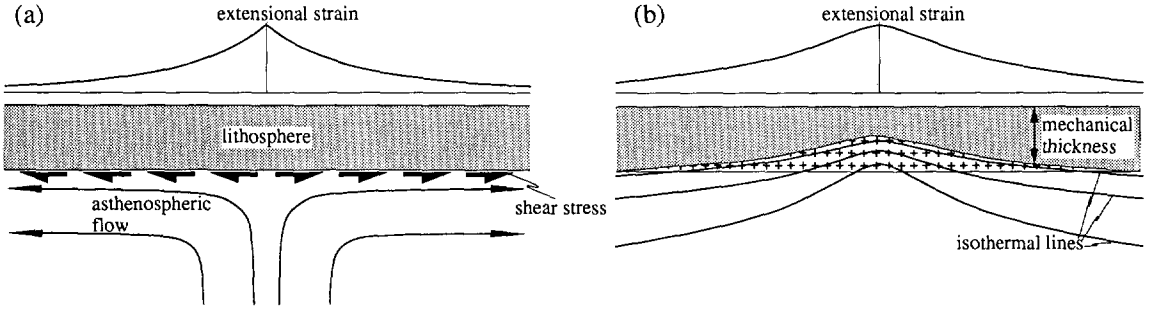

Fig. 10. Two plausible mechanisms to produce an extensional strain or stress gradient in the lithosphere: (a) by asthenospheric flow diverging laterally; and (b) by uneven mechanical thickness of the lithosphere due to the thermal gradient changing laterally.

thickness of the lithosphere, which is mainly due to the lateral change in thermal gradient. Even if the magnitude of extensional force is constant, the extensional stress and strain are maximum at the zone of highest thermal gradient (Fig. 10b).

It is unknown yet whether the driving force is due to active divergent lateral flows of asthenosphere during active rifting or divergent motions of two plates during passive rifting (Sengör & Burke 1978, Condie 1989), but the mechanical thickness of the lithosphere is certainly minimum at the axes of mid-oceanic ridges and rifts, for example the North Sea (Wood & Barton 1983, Barton & Wood 1984). It is highly probable that extensional strain is highest at the axis of an extensional tectonic zone. Not only mid-oceanic ridges (Harper 1985) but also some of the continental rifts, for example the North Sea rift (Day *et al.* 1981, Ziegler 1982b, Wood & Barton 1983), are associated with normal faults facing towards the rift axes. Such asymmetric faulting is thought to be a manifestation of the strain gradient in the lithosphere, suggesting that our experimental results are applicable to nature. Therefore, based on our experimental results, we conclude that the asymmetries of normal fault systems reflect the magnitude of extensional strain gradients.

Acknowledgements—We gratefully acknowledge helpful discussions and suggestions with two reviewers, Prof. K. R. McClay (University of London) and Dr R. J. Norris (University of Otago) on several points in this paper. Special thanks are also due to them for careful improvements of English.

REFERENCES

Allemand, P. & Brun, J. P. 1991. Width of continental rifts and rheological layering of the lithosphere. In: *Experimental and Numerical Modelling of Continental Deformation* (edited by Cobbold, P. R.). *Tectonophysics* **188**, 63–70.

Barton, P. & Wood, R. 1984. Tectonic evolution of the North Sea basin: crustal stretching and subsidence. *Geophys. J. R. astr. Soc.* **79**, 987–1022.

Brun, J. P. & Choukroune, P. 1983. Normal faulting, block tilting and décollement in a stretched crust. *Tectonics* **2**, 345–356.

Buchanan, P. G. & McClay, K. R. 1991. Sandbox experiments of inverted listric and planar fault systems. In: *Experimental and Numerical Modelling of Continenetal Deformation* (edited by Cobbold, P. R.). *Tectonophysics* **188**, 97–116.

Cheadle, M. J., McGeary, S., Warner, M. R. & Matthews, D. H. 1987. Extensional structures on the western UK continenetal shelf: a review of evidence from deep seismic profiling. In: *Continental Extensional Tectonics* (edited by Coward, M. P., Dewey, J. F. & Hancock, P. L.). *Spec. Publ. geol. Soc. Lond.* **28**, 445–466.

Condie, K. C. 1989. *Plate Tectonics and Crustal Evolution*. Pergamon Press, New York.

Crans, W., Mandl, G. & Haremboure, J. 1980. On the theory of growth faulting: A geomechanical delta model based on gravity sliding. *J. Petrol. Geol.* **2**, 265–307.

Day, G. A., Cooper, B. A., Andersen, C., Burgers, W., Ronnevik, H. & Schoneich, H. 1981. Regional seismic structure maps of the North Sea. In: *The Petroleum Geology of The Continental Shelf of N.W. Europe* (edited by Illing L. V. & Hobson G. D.). Hayden, London, 76–84.

Ellis, P. G. & McClay, K. R. 1988. Listric extensional fault systems—results of analogue model experiments. *Basin Res.* **1**, 55–70.

Harper, G. D. 1985. Tectonics of slow spreading mid-ocean ridges and consequences of a variable depth to the brittle/ductile transition. *Tectonics* **4**, 395–409.

Jaeger, J. C. & Cook, N. G. W. 1979. *Fundamentals of Rock Mechanics*. Chapman & Hall, London.

Kautz. S. A. & Sclater, J. G. 1988. Internal deformation in clay models of extension by block faulting. *Tectonics* **4**, 823–832.

Kirton, S. R. & Hitchen, K. 1987. Timing and style of crustal extension N of the Scottish mainland. In: *Continental Extensional Tectonics* (edited by Coward, M. P., Dewey, J. F. & Hancock, P. L.). *Spec. Publ. geol. Soc. Lond.* **28**, 501–510.

Liu, G. 1987. The Cenozoic rift system of the North China Plain and deep internal process. *Tectonophysics* **133**, 277–285.

Mandl, G. 1988. *Mechanics of Tectonic Faulting*. Elsevier, Amsterdam.

McClay, K. R. 1990a. Extensional fault systems in sedimentary basins: a review of analogue model studies. *Mar. Pet. Geol.* **7**, 206–233.

McClay, K. R. 1990b. Deformation mechanisms in analogue models of extensional fault systems. In: *Deformation Mechanisms, Rheology and Tectonics* (edited by Knipe, R. J. & Rutter, E. H.). *Spec. Publ. geol. Soc. Lond.* **54**, 215–227.

McClay, K. R. & Ellis, P. G. 1987a. Geometries of extensional fault systems developed in model experiments. *Geology* **15**, 341–344.

McClay, K. R. & Ellis, P. G. 1987b. Analogue models of extensional fault geometries. In: *Continental Extensional Tectonics* (edited by Coward, M. P., Dewey, J. F. & Hancock, P. L.). *Spec. Publ. geol. Soc. Lond.* **28**, 109–125.

McClay, K. R. & Scott, A. D. 1991. Experimental models of hanging-wall deformation in ramp–flat listric extensional fault systems. In: *Experimental and Numerical Modelling of Continental Deformation* (edited by Cobbold, P. R.). *Tectonophysics* **188**, 85–97.

McKenzie, D. P. 1978. Some remarks on the development of sedimentary basins. *Earth Planet. Sci. Lett.* **40**, 25–32.

Sengör, A. M. C. & Burke, K. 1978. Relative timing of rifting and volcanism on earth and its tectonic implications. *Geophys. Res. Lett.* **5**, 419–421.

Smith, R. B. & Bruhn, R. L. 1984. Intraplate extensional tectonics of the eastern Basin–Range: inferences on structural style from seismic reflection data, regional tectonics and thermal–mechanical models of brittle ductile deformation. *J. Geophys. Res.* **89**, 5733–5762.

Tron, V. & Brun, J. P. 1991. Experiments on oblique rifting in brittle–ductile systems. In: *Experimental and Numerical Modelling of Continental Deformation* (edited by Cobbold, P. R.). *Tectonophysics* **188**, 71–84.

Vendeville, B., Cobbold, P. R., Davy, P., Brun, J. P. & Choukroune, P. 1987. Physical models of extensional tectonics at various scales. In: *Continental Exensional Tectonics* (edited by Coward, M. P., Dewey, J. F. & Hancock, P. L.). *Spec. Publ. geol. Soc. Lond.* **28**, 95–107.

Vendeville, B. & Cobbold, P. R. 1988. How normal faulting and sedimentation interact to produce listric fault profiles and stratigraphic wedges. *J. Struct. Geol.* **10**, 649–659.

Wernicke, B. 1981. Low-angle normal faults in the Basin and Range Province: nappe tectonics in an extending orogen. *Nature* **291**, 645–648.

Wernicke, B. 1985. Uniform-sense normal simple shear of the continental lithosphere. *Can. J. Earth Sci.* **22**, 108–125.

Wernicke, B. & Burchfiel, B. C. 1982. Modes of extensional tectonics. *J. Struct. Geol.* **4**, 105–115.

White, N. & McKenzie, D. P. 1988. Formation of the "steer's head" geometry of sedimentary basins by differential stretching of the crust and mantle. *Geology* **16**, 250–253.

Wood, R. & Barton, P. 1983. Crustal thinning and subsidence in the North Sea. *Nature* **302**, 134–136.

Ziegler, P. A. 1982a. Faulting and graben formation in western and central Europe. *Phil. Trans. R. Soc. Lond.* A, **305**, 113–143.

Ziegler, P. A. 1982b. *Geological Atlas of Western and Central Europe*. Elsevier, Amsterdam.